Design Optimization of 12-Core Amplifier Based on Erbium Ytterbium Co-Doped Fiber for Spatial Multiplexed Transmission System

Aurélien Lebreton, Gilles Mélin, Sylvain Bordais, Romain Kerampran, Erwan Pincemin, Thierry Taunay, *Member, IEEE*, Jérémie Jauffrit, Pierre-Yves Disez, Claude Le Bouëtté, Yves Jaouën, Michel Morvan, and Chao Lu

***Abstract*—A 20 dB gain 12 cores Er^{3+}/Yb^{3+} co-doped cladding pumped amplifier in C-band with only 5.3 W of pump power has been achieved. A classical rate equation model has been applied for the amplifier design. Parameters such as active fiber length, pump power and ions concentration have been investigated and optimized. Results obtained through numerical simulation and experimental investigations are compared. Different use cases of MC-EYDFA have been studied, such as various transmission configuration or multi-core amplifier in ROADM architectures. 1200-km with 200G DP-QPSK and 300 km with 400G DP-16QAM are achieved in serial configuration at 1550 nm. This is a first step towards SDM transmission using power efficient amplifiers, for cost, energy and footprint saving.**

***Index Terms*—SDM, multi-core amplifier, erbium ytterbium co-doped fiber, PSO, 200G/400G transmission, cost and energy saving.**

Manuscript received 27 April 2022; revised 9 July 2022, 29 September 2022, and 21 October 2022; accepted 22 October 2022. Date of publication 26 October 2022; date of current version 15 January 2023. This work was supported by the BPI France, Région Bretagne, Lannion Trégor Communauté (LTC) and Direction Générale de l'Armement (DGA) France ("EFFLAM" project). *(Corresponding author: Yves Jaouän.)*

Aurélien Lebreton was with the LTCI, Télécom Paris, Institut Polytechnique de Paris, F-91120 Palaiseau, France. He is now with the Shenzhen Research Institute, Shenzhen Virtual University Park, Shenzhen 518057, China (e-mail: aurelien.lebreton@yahoo.com).

Gilles Mélin is with the iXblue, 22300 Lannion, France (e-mail: gilles.melin@ixblue.com).

Sylvain Bordais and Romain Kerampran are with the Lumibird, 22300 Lannion, France (e-mail: sbordais@lumibird.com; romain.kerampran@gmail.com).

Erwan Pincemin is with the Orange Labs, 22300 Lannion, France (e-mail: erwan.pincemin@orange.com).

Thierry Taunay was with the Photonics Bretagne, 22300 Lannion, France. He is now with the Lumibird, 22300 Lannion, France (e-mail: ttaunay@lumibird.com).

Jérémie Jauffrit, Pierre-Yves Disez, and Claude Le Bouëtté are with the Ekinops, 22300 Lannion, France (e-mail: jeremie.jauffrit@ekinops.com; pierre-yves.disez@ekinops.com; claude.leboutte@ekinops.com).

Yves Jaouën is with the LTCI, Télécom Paris, Institut Polytechnique de Paris, F-91120 Palaiseau, France (e-mail: yves.jaouen@telecom-paris.fr).

Michel Morvan is with the IMT Atlantique, 29280 Plouzané, France (e-mail: michel.morvan@imt-atlantique.fr).

Chao Lu is with the Hong Kong Polytechnic University, Hong Kong, and also with the Shenzhen Research Institute, Hong Kong Polytechnic University, Hong Kong (e-mail: chao.lu@polyu.edu.hk).

Color versions of one or more figures in this article are available at https://doi.org/10.1109/JLT.2022.3217308.

Digital Object Identifier 10.1109/JLT.2022.3217308

I. Introduction

THE capacity demand in communications is growing and is expected to increase exponentially in the foreseeable future. This growth of demand has stimulated development of different technologies to maximize system capacity. The transmission through single-mode fiber (SMF) is considered to achieve its capacity limit of ∼100 Tbs/s [1]. Therefore, the need of new technical approaches to overcome this limitation is required. Space is the last degree of freedom to be implemented in order to increase the upcoming capacity. Different Space Division Multiplexing (SDM) approaches have been proposed to overcome this limitation [2]. SDM fibers can be classified into three categories such as (a) multi-mode fiber (MMF), which utilizes more than one linearly polarized (LP) mode in a single core by enlarging the fiber core diameter, (b) multi-core fiber (MCF), where several cores coexist in the same cladding or (c) a combination of MMF with MCF. Many researches are carried out in improving the capacity of communication networks by using multiple independent cores per fiber [3], [4], [5], multiple modes per core [6], [7], a combination of both [8] or a coupled-core structure [9].

In Wavelength Division Multiplexing (WDM) systems, optical amplifiers are key system components as they allow a spectral sharing of the amplification function among a large number of channels. It then makes sense to study the benefit of Multi-Core Doped-Fiber Amplifiers (MC-EDFA)[10] to share the amplification function also in the spatial dimension. Having a single MC-EDFA for many fibers modes or cores instead of one standard Erbium Doped Fiber Amplifier (EDFA) per line will induce savings in terms of cost, energy consumption, and compactness [11]. Various multi-mode and multi-core optical amplification solutions have been studied over the past years [12], [13]. In the specific case of multi-mode amplification, there is a variation in gain and noise figure among the guided spatial modes of the LP type (LP_{01}, LP_{11}, LP_{21}, LP_{02}, etc...) taking into account the different pump-signal overlap integrals [14]. The multi-core amplification, has a number of advantages compared to the previous solution: no competition between the LP-guided modes, pooling of a single pump with low brightness but high power (i.e. via pumping by the cladding) [15]. Another big advantage of MC-EDFA is to be connectable to a fiber bundle

through fan-in/out devices, and thus to share the amplification function among a large number of standard single-mode fibers without changing the in-field fiber infrastructure.

In this paper, we will consider the design and optimization of a cladding pumped Multi-Core Erbium-Ytterbium Doped Fiber Amplifier (MC-EYDFA) [16], [17], [18]. The comparative advantages/disadvantages of Erbium (Er^{3+}) and Erbium/Ytterbium (Er^{3+}/Yb^{3+}) doping are relatively well-known [19]. An Er/Yb co-doped fiber amplifier provides higher gain and better pump efficiency than an Erbium amplifier. Indeed, pump absorption with a cladding pumping is low by considering only a Er^{3+} doping. Its results that high pump power is required for significant population inversion to allow WDM amplification in C-band. The pump absorption is much higher in the case of Er^{3+}/Yb^{3+} doping. Yb^{3+} ions concentration is about 10 time higher than that of Er^{3+}, resulting in higher conversion efficiency. In addition, the double-clad structure of the Er/Yb doped fibers combined with high power broad-area lasers source at 940 nm or 976 nm makes it possible to exceed the powers that can be envisaged with single-mode diodes at 980 nm. Some limitations of the design are: mandatory phosphorus doping for efficient ytterbium to erbium energy transfer which results in counterpart in reduced WDM amplification gain in the telecom C-band window [20]. Moreover, such Er^{3+}/Yb^{3+} fiber amplifiers present 2–3 dB higher noise figure compared to pure Er^{3+} fiber amplifiers, but this effect could be reduced through amplifier architecture optimization.

In the literature, it exists two distinct coupled multi-core fibers approaches. The first one, named strongly coupled multi-core fibers, deliberately reduce the core spacing, introducing inter-core crosstalk, resulting in supermode transmission. Its performance is better than equivalent single-mode fiber thanks to the strong random mixing between the cores, reduces the cumulative effect of non-linear effects but the cost of decoupling with Multiple-Input, Multiple-Output (MIMO) equalization at the receiver side is very high [21]. The second one, called weakly coupled multi-core fibers, consider that each core is independent. Core-to-core are sufficiently separated to minimize crosstalk. The advantage of this equalization is that it does not require complex MIMO. The following study has been based on that consideration for the MC-EYDFA amplifier design. Finally, note that the fiber bundle approach is technically the simplest because it generates the lowest impairments with no crosstalk or complex MIMO processing to be implemented on the receiver side.

In this paper, we will study the impact of using a MC-EYDFA in terms of performances, energy and cost saving compared to standard EDFA. We adapt the considered optical bandwidth in order to obtain best results in terms of NF and gain variation. We provide also some additional input by extending the C-band to the L-band through simulations. The paper is divided as follows. In Section II, the implemented multi-core amplifier technology is described. In Section III, we introduce the developed simulation tool to determine the optimal Er/Yb doped fiber intrinsic parameters as well as to predict the amplifier behaviors. Section IV, presents the fiber and amplifier characterization. Finally, Section V presents the contribution of mutualized MC-EYDFA in transmission systems and ROADM architectures. A techno-economic analysis is also carried out to give some perspectives on the potential use of such technology. Finally, the use of such amplifier for submarine transmission system is investigated.

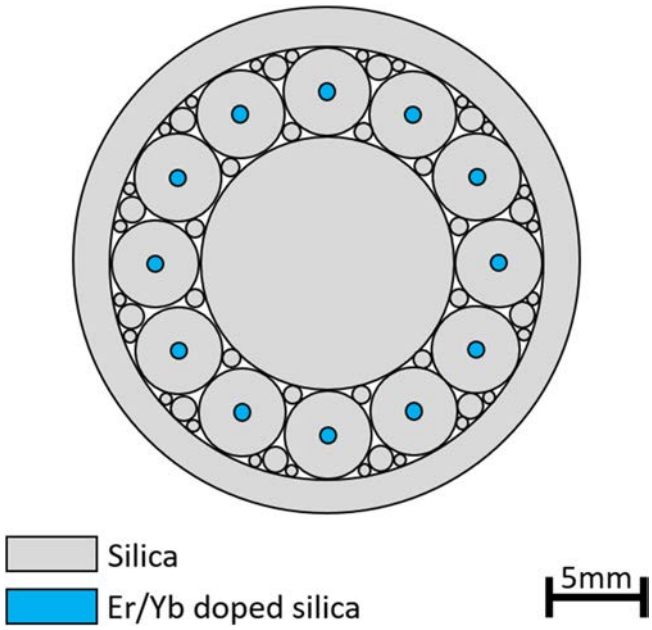

Fig. 1. Multi-Core preform design.

II. Multi-core Optical Amplifier Technology

A. Architecture Assembly

This part will present the architecture assembly of the multi-core fiber. Optical cables are typically arranged by 12-fibers clusters. Different geometries of core distribution in the cladding have been proposed: scalar [22] and hexagonal fiber array [23], or cores regularly arranged on a circle [24].

In our case, the 12c-EYDF design is based on the following considerations. Preforms can be implemented using the versatile stack-and-draw technique initially developed for photonics crystal fibers. As accuracy and stability of core-to-core spacing are crucial to reduce splicing losses between MCF and bundles, a preform design based on a circular arrangement of 4.1 mm rod which include Er^{3+}/Yb^{3+} doped cores around a central undoped 12 mm rod has been considered. The preform design is shown in Fig. 1. Erbium/Ytterbium doped fibers have been fabricated by Modified Chemical Vapor Deposition (MCVD) process using conventional solution doping process. Er/Yb doped core and external rod diameters suitable for preform assembly are obtained by additional glass work operations. After the stacking process, the 12 cores fiber with 6 μm diameter was realized in two steps to obtain the required average core-to-core spacing of 35 μm. A dual primary low index/secondary high index coating is used to get a numerical aperture of 0.48 for the 187.5 μm in diameter multimode clad.

The addition of the Ytterbium co-dopant makes it possible to have a fairly large absorption cross section but also a large absorption band ranging from 910 nm to 980 nm with a maximum peak at 976 nm. Gain and absorption spectrum for the considered co-doped Er^{3+}/Yb^{3+} fiber is calculated from the cross sections

Fig. 2. (a) Packaging of the combiner/fan-in spliced to the 12c-EYDF - (b) Cross view of the bundle.

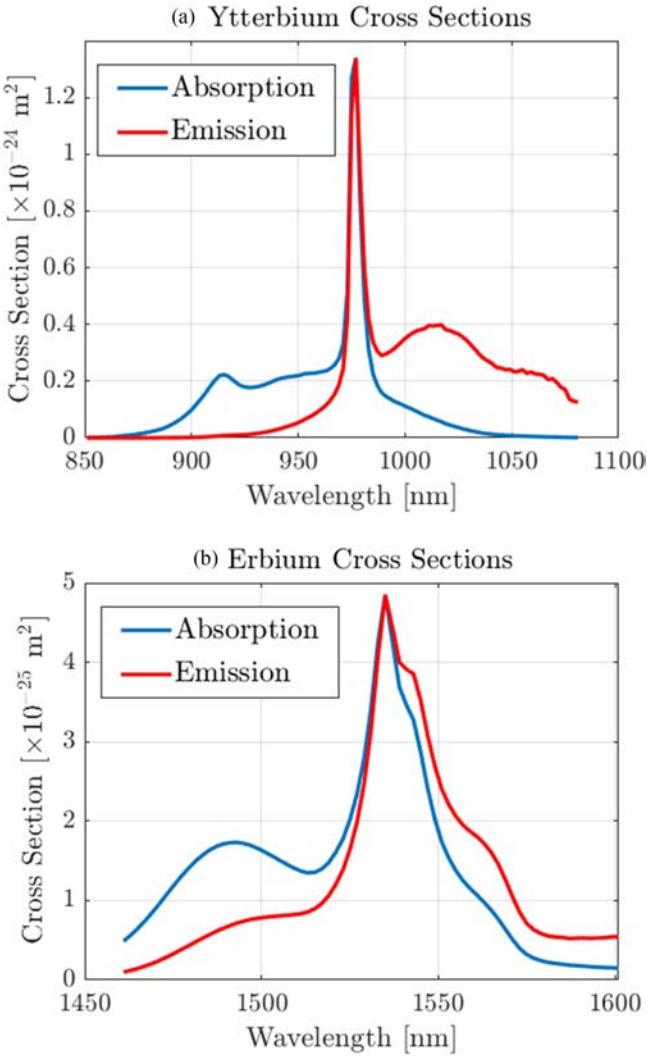

Fig. 3. Cross Sections of the considered Er-Yb fiber.

depicted on Fig. 3 and the concentration of ions. Concentration of Erbium and Ytterbium are key elements that will be further discuss in Section III.

The doped cores are surrounded by a large 1^{st} multimode cladding into which the pump light is launched. The pump light propagates in the multimode cladding which acts both as waveguide for the pump and as a cladding for the active single mode cores. The pump crosses the active cores where it is absorbed.

In the cladding-pumped multi-core amplification, which is considered here, the inter-core crosstalk is in general non-negligible and should be taken into consideration. The amplifier length and the non-uniform gain distribution over cores could have additional impact on the measured crosstalk, that could theoretically be in range of -60 dB/km to -30 dB/km [25]. Based on theoretical expression of crosstalk estimation derivated for multi-core amplifiers in [25], (6), we can consider that a core-to-core spacing of 35 μm induces low cosstalk. Results of measured crosstalk are discussed in Section IV.

B. Development of Combined Bundle/Fan Technology

The designed amplifier considers pump and signals into the 12c-EYDF using a tapered fiber bundle based combiner. It consists in 12 $\times$ 15 μm/80 μm fibers around a central 195/230 μm multimode fiber. The taperization process reduces the fibers cores to 6 μm diameter. The pump light is launched through the central 195/230 μm fiber. Reproducible core-to-core distances of $35 \pm 0.5\ \mu m$ are obtained, leading to a satisfactorily accurate matching to the 12c-EYDF geometry. An 15 μm/80 μm fiber with NA $= 0.19$ is multimode at 1550 nm. An $\sim$5 cm length section is spliced to an G.652 compliant type fiber. The output beam is measured using an infrared camera. The transverse alignment between the two fibers is optimized as the signal beam excite the fundamental LP_{01} mode only. As the multimode fiber section with straight alignment is only $\sim$5 cm, propagation in LP_{01} could be preserved. The overall package lead to keep a very short section of the multimode fiber in a straight line, reducing detrimental effects as mode mismatch due to micro-curvature. Fig. 2(a) presents the developed bundle and Fig. 2(b) the 12c-EYDF cross-section obtained by optical microscopy [26].

III. Multi-Core Er/Yb Doped Fiber Design

A simulation model has been used in order to determine the optimum intrinsic parameters to design the multi-core fiber, such as dopant concentration and active fiber length, to minimize NF and gain variation for a long distance transmission configuration targeted a gain of 20 dB and by considering a composite input power of 0dBm. The composite input power corresponds to the total input power per core considering all WDM channels.

A. Modeling of MCF-Based Amplifier

For simplicity, the simulation model considers only one core and one clad to simulate 12 cores amplifier. We assume to modify the ratio of the areas between the cladding and the core to simulate the equivalent of a 12-core fiber as calculated in (1). This assumption is based on an uniform pump distribution in the cladding. It is reasonably accurate thanks to the high-index cores which mixed well the spatial modes. The accuracy of the assumption has been previously investigated in [27].

$$R_s = \frac{S_{core}}{S_{clad}/N_{core}} = \frac{d_{core}^2}{d_{clad}^2/N_{core}} \tag{1}$$

with S, d and N, the area, diameter and number of core respectively.

The simulation tool is based on the equations model initially developed for EDFA [28]. A classical two levels Er^{3+}/Yb^{3+} transfer energy system has been considered, including cooperative up conversion process due to high ions concentrations [29]. The population inversion fraction is determined by solving the rate equations for Er^{3+} and Yb^{3+} ions, taking into account the pump, signal and Amplified Spontaneous Emission (ASE) powers evolution as express in from (2) to (4).

$$\frac{dP_p^{\pm}}{dz} = \pm\left[\left(\alpha_{Yb}+\gamma_{Yb}\right)n_{Yb} - \left(\alpha_{Yb}+l_{clad}\right)\right]P_p^{\pm} \quad (2)$$

$$\frac{dP_s(\nu)}{dz} = \left[\left(\alpha_{Er}+\gamma_{Er}\right)n_{Er} - \left(\alpha_{Er}+l_{core}\right)\right]P_s(\nu) \quad (3)$$

$$\frac{dP_{ASE}^{\pm}(\nu)}{dz} = \pm\left[\left(\alpha_{Er}+\gamma_{Er}\right)n_{Er} - \left(\alpha_{Er}+l_{core}\right)\right]P_{ASE}^{\pm}(\nu) \pm 2h\nu\Delta\nu\gamma_{Er} \quad (4)$$

where $P_p^{\pm}$, P_s and $P_{ASE}^{\pm}$ are the evolution of the pump, signal and ASE power respectively along the considered fiber. The $\pm$ expresses the forward $(+)$ and backward $(-)$ propagation. α and γ are the absorption and gain coefficient. l_{clad} and l_{core} are the background losses in the cladding and in the core respectively. n_{Er} and n_{Yb} are the normalized Erbium and Ytterbium ions population in the excited state respectively. $\Delta\nu$ is the considered optical resolution bandwidth expressed in frequency domain. h is the Planck constant. ζ_{Er} and ζ_{Yb} are the saturation parameter and C_{Er} is a constant that takes cooperative up-conversion phenomenon into account [30].

In a stationary regime, the normalized expressions of fractions of population inversions can be written as follows in (5) and (6) [29].

$$n_{Yb} = \frac{\alpha_{Yb}\dfrac{P_p}{h\nu_p\zeta_{Yb}}}{1+\left(\alpha_{Yb}+\gamma_{Yb}\right)\dfrac{P_p}{h\nu_p\zeta_{Yb}}+\kappa_{Yb}\left(1-n_{Er}\right)} \quad (5)$$

$$n_{Er} = \frac{\alpha_{Er}\dfrac{P_s}{h\nu_s\zeta_{Er}}}{1+\left(\alpha_{Er}+\gamma_{Er}\right)\dfrac{P_s}{h\nu_s\zeta_{Er}}+\kappa_{Er}n_{Yb}+C_{Er}n_{Er}} \quad (6)$$

Rate evolution equations are solved using ODE45 solver integrated in Matlab. $P_s(\nu)$ and $P_{ASE}^{\pm}(\nu)$ are calculated using a spectral resolution of 0.1 nm. The objective is to find the best amplifier parameters that maximize the gain, reduce the NF while saving energy. Parameters that need to be defined and optimized are listed below:

- Doped fiber length
- Input optical power
- Forward pump power
- Backward pump power
- Erbium and Ytterbium ions concentration
- Ratio of ion concentration Ytterbium/Erbium

Results of simulation will be focused on:

TABLE I
SIMULATIONS PARAMETERS VALUES

Symbol	Parameter	Value	Unit
Φ_{core}	Core Diameter	6	μm
Φ_{clad}	Clad Diameter	187.5	μm
Γ	Sig. Mode Overlap	0.76	
N_{Er}	Er Concentration	1.65×10^{25}	m^{-3}
N_{Yb}/N_{Er}	Yb/Er Ratio	[10 - 80]	
$\sigma_{Yb,e}$	Yb Cross Sec. Ems.	Fig. 3-a	m^2
$\sigma_{Yb,a}$	Yb Cross Sec. Abs.	Fig. 3-a	m^2
$\sigma_{Er,e}$	Er Cross Sec. Ems.	Fig. 3-b	m^2
$\sigma_{Er,a}$	Er Cross Sec. Abs.	Fig. 3-b	m^2
α_{Yb}	Yb Abs. Coeff.	$N_{Yb}\sigma_{Yb,a}R_s$	m^{-1}
α_{Er}	Er Abs. Coeff.	$N_{Er}\sigma_{Er,a}\Gamma$	m^{-1}
γ_{Yb}	Yb Ems. Coeff.	$N_{Yb}\sigma_{Yb,e}R_s$	m^{-1}
γ_{Er}	Er Ems. Coeff.	$N_{Er}\sigma_{Er,e}\Gamma$	m^{-1}
τ_{Yb}	Yb Lifetime	1.5	ms
τ_{Er}	Er Lifetime	11	ms
A	Effective Area	$\pi\left(\Phi_{core}/2\right)^2$	μm^2
ζ_{Er}	Er Sat. Param.	A N_{Er}/τ_{Er}	1/(m.s)
ζ_{Er}	Yb Sat. Param.	A N_{Yb}/τ_{Yb}	1/(m.s)
C_{Er}	Upconversion	2×10^{-23}	m^3/s
k_{tr}	Yb/Er Transf. Rate	3.5×10^{-22}	m^3/s
κ_{Yb}	Yb energy Exch. Par.	$k_{tr}N_{Yb}\tau_{Yb}$	
κ_{Er}	Er energy Exch. Par.	$k_{tr}N_{Er}\tau_{Er}$	
N_{core}	Number of Core	12	
l_{core}	Core Background Loss	30	dB/km
l_{clad}	Clad Background Loss	194	dB/km
λ_s	Signal Wavelength	[1535-1565]	nm
λ_p	Pump Wavelength	940	nm

- Minimize the noise figure of the amplifier
- Optimize the gain
- Optimize output power
- Minimize gain variation between upper and lower side of the optical spectrum (i.e. $\Delta G = G_{\max} - G_{\min}$, in dB)
- Minimize the power consumption

Simulations described in the next part will be based on the fiber cross sections values depicted on Fig. 3. The set of cross sections data used in the simulations were provided by iXblue and were measured on a commercially available equivalent single core Erbium-Ytterbium fiber.

Table I presents the used simulation parameters values. The first parameter that need to be determined is N_{Er} and N_{Yb} for Erbium and Ytterbium ions concentrations respectively and in particular the ratio between the two concentrations define as N_{Yb}/N_{Er}. For that, Erbium concentration is fixed to 1.65×10^{25} and that of Ytterbium varies. The used concentration of N_{Er} is typical of a range of commercially available Er/Yb fiber from the iXblue offer, notably the low noise figure of 6 μm core fiber.

To determine the best ions concentration ratio, we plot the signal gain, NF, output power and gain variation along a [1535–1565] nm optical bandwidth considering ratio and active fiber length as variables. The ratio of concentration varies from 10 to 80 for a fiber length between 3 and 6 meters as shown in Fig. 4. For each point, gain and absorption in the core and cladding

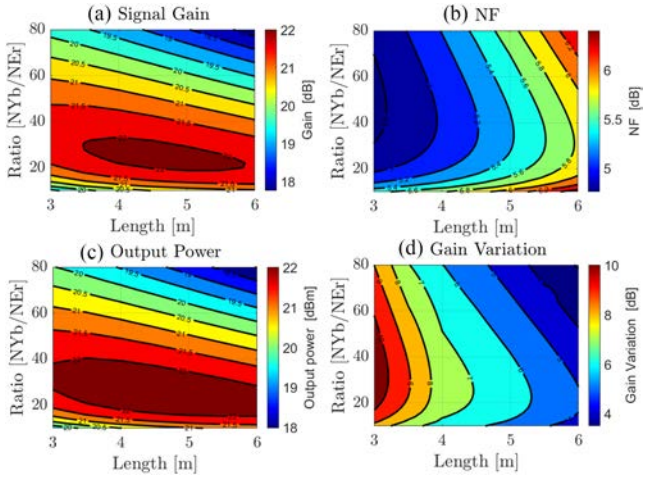

Fig. 4. (a) Gain, (b) NF, (c) Output Power and (d) Gain variation of the MC-EYDFA for different concentration ratio and active fiber length - Composite input power: 0 dBm, Backward pump power: 7.6 W.

are calculated based on ions concentrations values and the fiber cross sections of Fig. 3.

From these simulations results, we can determine the best fiber length and concentration ratio that will minimize both NF and gain variation values. To obtain those results, pump power has been fixed to 5.3W. Influence of the pump power will be later studied. From Fig. 4(b), we can observe that minimizing NF implies the selection of an active fiber length of 3m, for example, with a concentration ratio equal to 20. However, with these parameters, gain variation, in Fig. 4(d), is not minimal. Indeed, we can see that minimizing the NF imply to have an important gain variation and, to the opposite, minimizing the gain variation imply high NF values. As the results for these two functions evolve in opposite direction, we elaborate an algorithm based on Particle Swarm Optimization (PSO) to determine the best compromise point.

B. Pseudo-Swarm Optimization Technique

Traditional problems studied by PSO method have equations to be solved. In our case, we have no equation but finite number of points (i.e. Fig. 4) in which one we based our algorithm. In PSO terms, we consider a multi-objective optimization defined by:

- Objective functions: Gain, NF, Output Power and Gain variation simulation results (i.e. Fig. 4).
- Optimization criteria: Consider gain maximization, NF and gain variation minimization to be optimized simultaneously.
- Boundaries limits: considered active fiber length and ions concentration ratio.

The basis framework of implemented multi-objective PSO (MOPSO) is described in Algorithm 1:

In PSO terminology:

- *Particle*: represent a point in the solution space, here in $\mathbb{R}^3$.
- *Swarm*: Population or group of particles. PSO is a population based algorithm, which uses a large population of particles to search for good solutions simultaneously

Algorithm 1: Multi-Objective PSO Framework.

```
P ← Particle Initialization
A ← Create Archive
while Stopping criteria not satisfied do
    P ← Evaluate(P)
    A ← Update(A)
    P ← Select P_{best,i}
    P ← Select P_{best,g}
    P ← Update(P)
end while
```

- $P_{best,i}$: Best position of the particle i in the research area.
- $P_{best,g}$: The best position among all the particles in the group.

MOPSO is a computational method that optimizes a problem by iteratively trying to improve a candidate solution (swarm) with regard to a given measure of quality. It solves a problem by having a population of local solutions (pbest), and moving these optimum points around in the search-space according to simple mathematical formula [31]. Local best point is guided toward the best-known positions in the search-space, which are updated as better positions are found by other local best solution. This is expected to move toward the best compromise solution ($P_{best,g}$) [32]. The Hausdorff metric, that measure the distance between the current evaluated $P_{best,g}$ solution compared to the archived one, is used as convergence criteria. If this value is smaller than epsilon, here $\epsilon = 1.10^{-6}$, algorithm converge. A swarm particle algorithm is characterized by:

- N_{swarm}: A number of particles.
- $V_{\max}$: The maximum velocity of each particle i.
- w: The particle inertia, equal to 1.
- c_1 & c_2: The cognitive and social component respectively, used for weighting the conservative behavior (the tendency to return to the personal best solution visited) and the predisposition to follow the tendency of the group. Both coefficient are equal to 2.

Each particle is characterized at the iteration *t* by:

- $X_i(t)$: its position in the exploration space.
- $V_i(t)$: its speed.
- $P_{best,i}$
- $P_{best,g}$

(7) and (8) provide the expressions of the updated position and velocity of each particle i at each iteration t:

$$X_i(t+1) = X_i(t) + V_i(t+1) \tag{7}$$

$$V_i(t+1) = w.V_i(t) + c_1.rand_1\left(P_{best,i} - X_i(t)\right) + c_2.rand_2\left(P_{best,g} - X_i(t)\right) \tag{8}$$

After computation, the optimal solutions are ranked according to their relative performance in an ascending order for each objective. These ranks are then sorted and stored in a matrix such that it may be used to rank the fitness of the population, with the most fit being the solution that achieves the highest rank most often. Based on that matrix, a Pareto Front is calculated. These Pareto-optimal solutions are shown in Fig. 5.

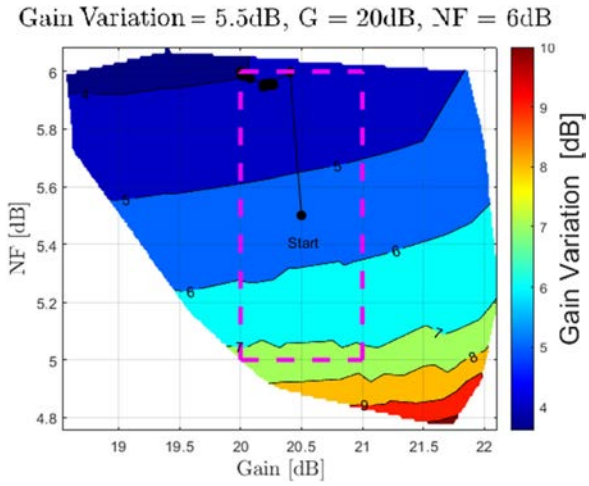

Fig. 5. 3D Pareto Front Solutions for $\lambda = 1550$ nm - Composite input power: 0 dBm, Backward pump power: 5.3 W.

Here, X-axis represents the gain, Y-axis represents the NF and range color represent the gain variation. Each point in this figure is a compromise that minimizes the NF and the gain variation parameters at the same time.

To determine the best solution, we set the output gain in the range of 20–21 dB. From Fig. 5 we can see that minimizing the NF will negatively affect the gain variation and vice versa. The algorithm determines the final point which minimize the NF without degrading too much the gain variation and reciprocally. The result give the optimum intrinsic parameters to design the amplifier for an output gain of 20 dB @1550 nm. Here the active fiber length and the ion concentration ratio should be 5.5 m and 20 respectively. In these simulations, a backward pump power equal to 5.3 W has been considered.

To further investigate the pumping impact on the NF and gain variation results, we add a forward pump in the model. The backward pump varies from 3 to 9 W and the forward pump from 0 to 6 W. Fig. 6 presents the results. If we look at Fig. 6(b), by modifying the ratio between forward and backward pump, for example 5.3 W can be rearrange in a 4 W backward pump and 1.3 W forward pump, NF is reduced by 0.2 dB (magenta dot arrow). We can furthermore improve NF by using 4.2 W backward pump and 1.8 W forward pump. In that case, we increase the total pump power but the NF is reduced by 0.4 dB (magenta solid arrow). In both conditions gain is kept constant at 20 dB, Fig. 6(a), and gain variation does not vary significantly (+0.1 dB for the worse case). Through this simulation, we can see that it is possible to reduce the noise figure of the amplifier by correctly selecting backward and/or forward pump power configuration.

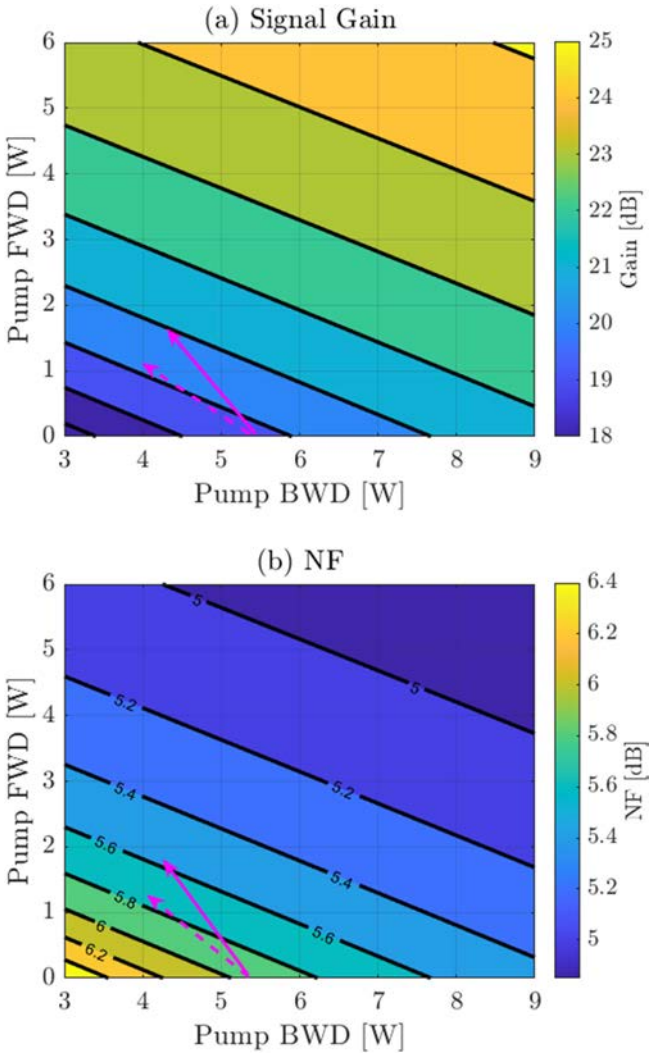

Fig. 6. (a) Gain and (b) NF as function of Backward (BWD) and Forward Pump (FWD) - Composite input power: 0 dBm, Fiber Length: 5.5 m, λ: 1550 nm.

IV. Multi-core Amplifier Fabrication

A. Considered Er/Yb Doped Fiber

Based on the simulations presented in Section III, a MC-EYDFA has been designed and manufactured [33]. Table II summarize the final optimal intrinsic fiber parameters. Core and clad diameters are respectively 6 and 187.5 μm. For a 20 dB gain at 1550 nm, the ratio between Ytterbium and Erbium ions concentration should be 20.

TABLE II
Final Er/Yb Doped Fiber Parameters Values

Symbol	Parameter	Value	Unit
Φ_{core}	Core Diameter	6	μm
Φ_{clad}	Clad Diameter	187.5	μm
α_{Yb}	Clad Abs. @914nm	3.7	dB/m
α_{Er}	Core Abs. @1534nm	42.3	dB/m
N_{Er}	Er Ion Concentration	1.65×10^{25}	m^{-3}
N_{Yb}/N_{Er}	Concentration Ratio	20	

Fig. 7(a) presents the optical microscopy picture of the considered 12c-EYDF while Fig. 7(b) show the pump distribution in the active fiber. We can observe the good pump distribution, validating the assumption made in Section II, (1).

Core-to-core spacing is found to be $35.0 \pm 0.3 \mu$m using a calibrated optical microscope. This result highlights the tight

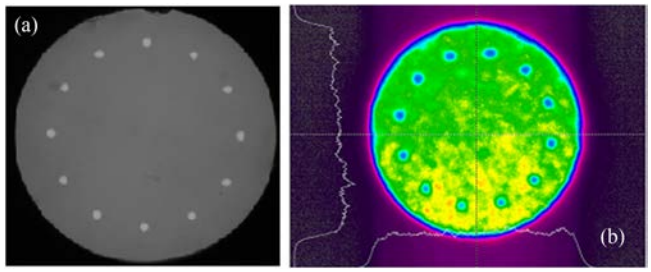

Fig. 7. (a) Optical microscopy picture of the 12c-EYDF (Core Diameter = 6 μ m, NA = 0.19, Core to Core distance = 35 μm) - (b) Er/Yb Doped fiber pump distribution.

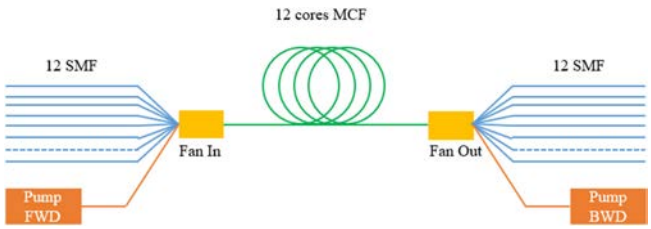

Fig. 8. 12 Cores Amplifier Architecture.

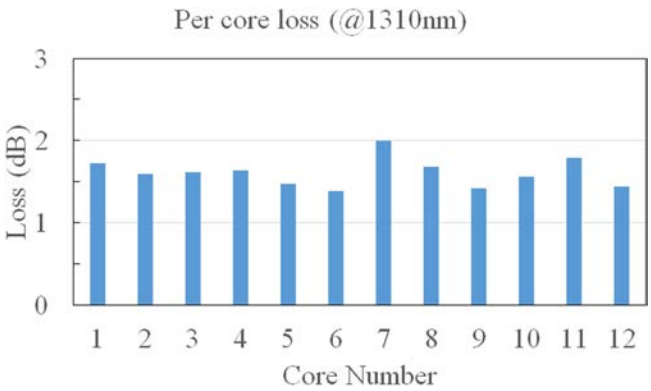

Fig. 9. End-to-end loss measurement for each core.

geometrical tolerance obtained on the cores positioning. Erbium and Ytterbium absorptions have been measured by the cut-back method using a broad-band source launched into the multimode clad. Total rare-earth clad absorptions are estimated to be 3.7 dB/m and 0.53 dB/m, respectively at 914 nm and 1534 nm.

B. Multi-Core Fiber Characterization

Fig. 8 presents the 12c-EYDF directly spliced, at both ends, to two 12+1 combiners. The fiber cleave angle is found to have a critical impact on the coupling loss and should be maintained below 0.1 deg. The Fan-In/Fan-Out (FIFO) combiners are first characterized by measuring total signal loss at 1.3 μm when spliced to a 5.5 m long 12 core fiber.

From Fig. 9, an averaged insertion loss of 1.7 dB is obtained with $\pm$0.3 dB core-to-core variations. This value includes 0.45 dB for each pigtails and 0.5 dB for fiber intrinsic attenuation at 1.3 μm. The latter has been estimated from optical time domain reflectometry measurements over a long length of 12c-EYDF.

TABLE III
INTRINSIC AMPLIFIER PARAMETERS

Symbol	Parameter	Value	Unit
L	Active Fiber Length	5.5	m
P_{FWD}	Forward Pump Power	0	W
P_{BWD}	Backward Pump Power	5.3	W
P_{in}	Composite Input Power	0	dBm
λ_s	Signal Wavelength	[1535-1565]	nm

C. Amplifier Characterization

This part will detail the amplifier characterization. Table III summarize the principal amplifier parameters.

A 940 nm multimode pump laser diode is chosen as it relaxes diode cooling requirements as the pump absorption is relatively temperature insensitive in this wavelength range [34]. 5.3 W pump power is injected into 5.5 m long 12 cores co-doped fiber via end-coupling in a counter-directional pumping configuration, with an efficiency $>$99%. Individual core performances are measured by launching 15 WDM channels spanning from 1535.2 nm to 1564.1 nm, with 0 dBm per channel input power launched into each core. The comparison between the simulations and experimental results in terms of gain per wavelength and NF is shown in Fig. 10.

Blue curves are the average experimental results and dotted magenta are for simulations. We can observe, from these figures, a good agreement between simulations and experimentation. Averaged over all the cores and all the wavelengths gain is 19 dB. Gain variation is 6 dB from 1535 nm to 1562 nm. NF and gain at 1550 nm are respectively 6 dB and 20 dB. This values are in agreement with PSO simulation results detailed in Fig 5.

Fig. 11 exposes the measured per core optical output power versus pump power. We can see that maximal core-to-core output power variation is only of 1.4 dB. Core-to-core crosstalk is evaluated by injecting signal power in one core and measuring power at the output of one of the two adjacent cores. The measured crosstalk varies from 33 to 42 dB over all cores, which is sufficient to prevent system performance impairments.

D. Power Consumption

We compare the total power consumption required for laser diodes operation and cooling in conventional single mode EDFAs and the proposed cladding pumped 12c-EYDFA. In conventional single mode EDFAs, a typical pump diode consumes an average of 1.6 W of electrical power for an output pump power of about 400 mW, sufficient to provide about 20 dBm of saturated output power. To operate at this power level, around 1.8 W of electrical power is needed to actively cool the diode and to maintain its temperature (assuming a state-of-the-art low power consumption diode [35]). This would lead to a total power consumption of about 40.8 W for 12 amplifiers. In the case of the studied 12c-EYDF, we use a total coupled pump power of 5.3 W

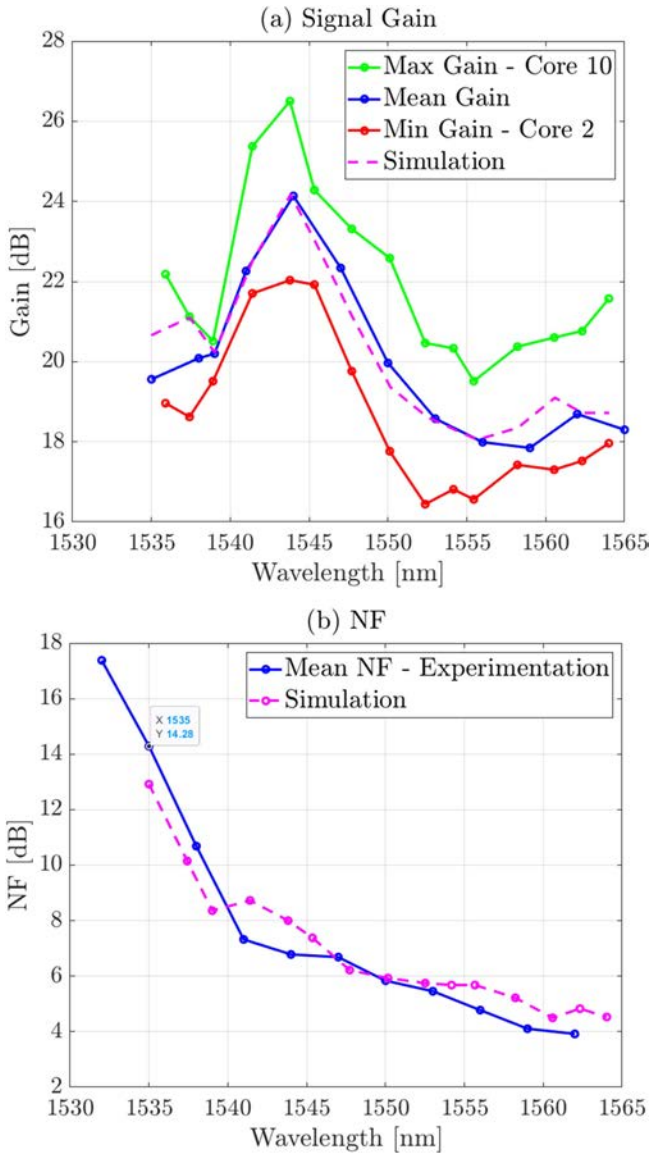

Fig. 10. Simulation and experimental results comparison. (a) Gain, (b) NF versus wavelength.

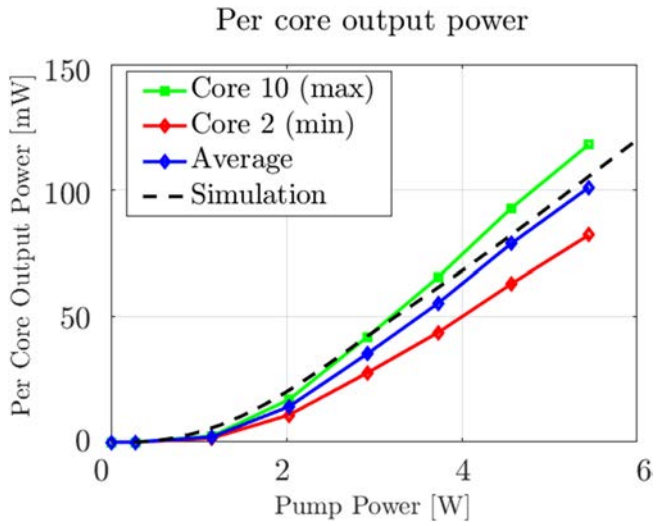

Fig. 11. Output power versus pump power - max, min, average and simulation comparison.

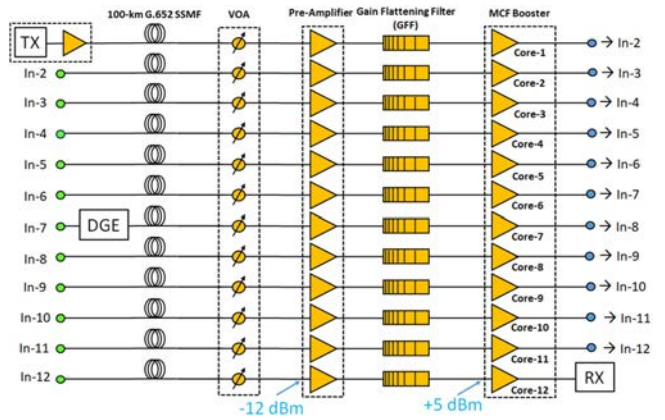

Fig. 12. First stage amplification (Single Mode EDF pre-amplifier + Gain Flattening Filter).

with a 99% pump coupling efficiency. On the other hand, optical efficiency of our multimode pump laser diodes is about 50%. Using those figures, the total electrical power consumed in our 12-core EYDFAs is about 10.7 W. This comparison highlights that our 12c-EYDFA architecture has the potential to provide significant power saving benefits.

V. Contribution of Multi-Core Amplifier in Transmission Systems

This section presents, first, an experimental demonstration of MC-EYDFA in a WDM transmission system. Then, some use cases are suggested by integrating multi-core amplifier in SDM architectures. A study on cost and energy consumption is then delivered. Finally, some perspectives on using such amplifiers in submarine system are discussed.

A. Transmission System Using Multi-Core Amplifier

In this section we will present the experimental results of using the designed amplifier in a WDM transmission system testbed. To assert the MC-EYDFA performance along its various cores, it can be interesting to concatenate the amplifiers (or cores) the ones behind the others with standard single-mode fiber spans between them, as we will do in a multi-span WDM transmission experiment with SC-EDFA. Another interesting use case is to insert the MC-EYDFA in an experiment that reproduces a data center interconnect (DCI) scenario where the 400G data flows are sent on parallel single-core single-mode fiber and amplified in the MC-EYDFA.

1) Multi-Span WDM Experiment Using the Multi-Core Amplifier: The experimental set-up is shown in Fig. 13. The WDM transmitter is made of two 200G/400G DP-QPSK/DP-16QAM interfaces at 1549.32 nm and 1550.12 nm, and 50 additional 100G DP-QPSK channels ranged from 1535.8 to 1557 nm on the 50 GHz ITU-T grid. The first 200G/400G interface is a ZR+ DCO-CFP2 (Digital Coherent Optics - Cent Form factor

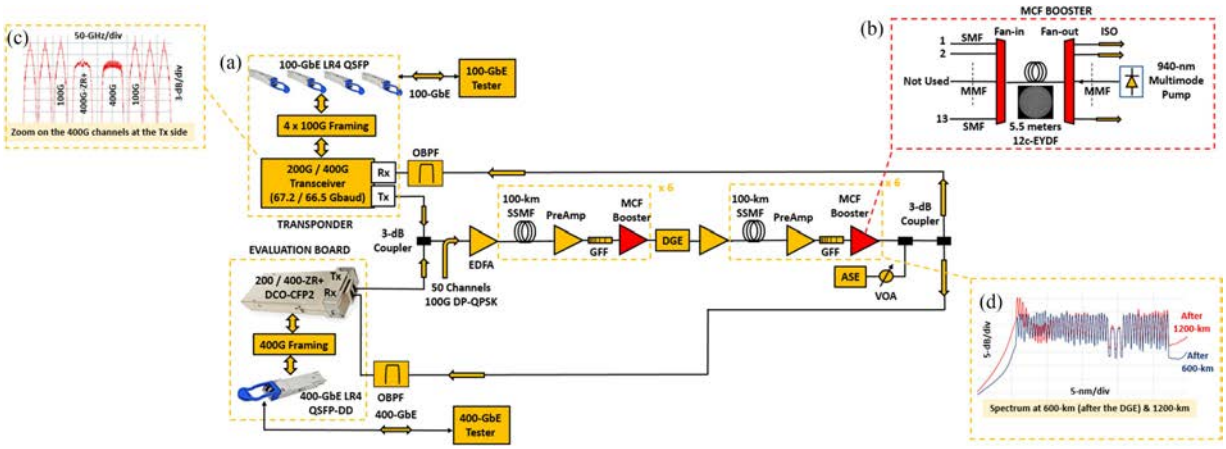

Fig. 13. (a) Set-up of the transmission experiment, with the 200/400G-ZR+ DCO-CFP2 transceiver, the proprietary 200G/400G transponder, the 52 DP-QPSK channels at 100 Gbps, and the 12 × 100 km ITU-T G.652 fiber line including the 12c-EYDF amplifier. (b) 12c-EYDF amplifier architecture. (c) Zoom over the WDM multiplex where are located the 200G/400G signals under test at the transmitter output. (d) Spectrum of the WDM multiplex at 600 km after the DGE (blue) and 1200 km (red).

Pluggable generation 2) operating at 60.1 Gbaud with the standardized O-FEC [36]-[38]. The second interface is a proprietary transponder working with a Low Density Parity Check (LDPC) Forward Error Correction Code (FEC) working with a total baud rate of 67.2/66.5 Gbaud. A zoom over the WDM multiplexed channels with the 200G/400G signals under test is shown in Fig. 13(c).

The uncompensated chromatic dispersion 1200 km transmission line is constituted of twelve 100 km spans of ITU-T G.652 fiber. Double-stage amplifiers compensate for the span losses. The first stage is a conventional single-mode EDF pre-amplifier with noise figure of ∼5 dB followed by a gain flattening filter (GFF) and the 12c-EYDF amplifier used as a second stage or booster with 5.3 W as pump power as depicted on Fig. 12.

To ensure a flat gain over the spectral region targeted for the [pre-amplifier + GFF + MCF amplifier] ensemble, the power at the pre-amplifier input had to be tuned to −12 dBm thanks to a VOA located just before the pre-amplifier stage. A dynamic gain equalizer (DGE) is inserted in the middle of the link. The WDM multiplex spectrum measured at 600km (after the DGE) and 1200 km is shown in Fig. 13(d).

At the receiver side, the 200G/400G channels are separated by two 80 GHz square flat-top optical band-pass filters (OBPF) and sent into the DCO-CFP2 receiver and the proprietary transponder respectively. As shown in Fig. 13(a), the evaluation board that embeds the DCO-CFP2 module, and the proprietary transponder are equipped to host respectively one client 400GbE LR4 QSFP-DD (Quad Small Form Factor Pluggable Double Density) interface and four client 100GbE LR4 QSFPs (directly connected to 400GbE and 100GbE testers). The post-FEC errors can thus be measured and error-free operation of the configurations under test identified.

Fig. 14 presents the results obtained using this configuration operating at 200G and 400G [39]. It appears that the FEC limit (BER $\sim 2.10^{-2}$) at ∼1550 nm is reached after only 300km at 400G with a received OSNR of 22 dB. Switching to 200G greatly relaxes the transmission constraints and allows achieving 1200 km with a received OSNR of ∼13.5 dB.

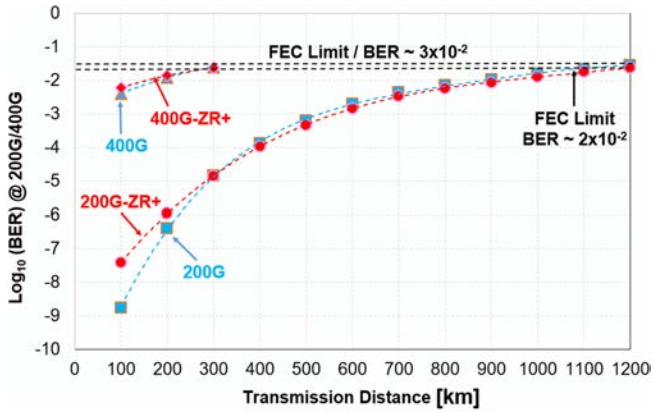

Fig. 14. BER vs. transmission distance at 1550 nm for the 200G/400G interfaces under test in the serial configuration.

In Fig. 15, we measure the performance of 200 G/400 G channels for the proprietary transponder when wavelengths are varied from 1535.8 to 1557 nm by step of 150-GHz. BERs and OSNRs are plotted as a function of wavelengths. It appears that the distance has to be reduced to 600 km at 200 G and 200 km at 400 G to have an error-free behavior for all the bandwidth. In particular, the lowest wavelengths show an OSNR reduction of 5 dB at 200 G and 3.5 dB at 400 G compared to the longest wavelengths.

2) Data Center Interconnect (DCI) Experiment Using the Multi-Core Amplifier: In the previous section (Fig. 12), the MC-EYDFA has been used in a 1200 km (i.e. 12 × 100 km) serial transmission set-up (for simulating a metro/regional scenario). In this section, the MC-EYDFA is used in a parallel configuration for reproducing data center interconnect (DCI) application. The experimental set-up is presented in Fig. 16.

The WDM transmitter is identical to the one previously described except that only 400 G data flows are considered here coming either from the 400 G-ZR+ pluggable optics or from the 400 G proprietary transponder. A 23 dBm standard EDFA amplifies the WDM multiplex previously described before a two

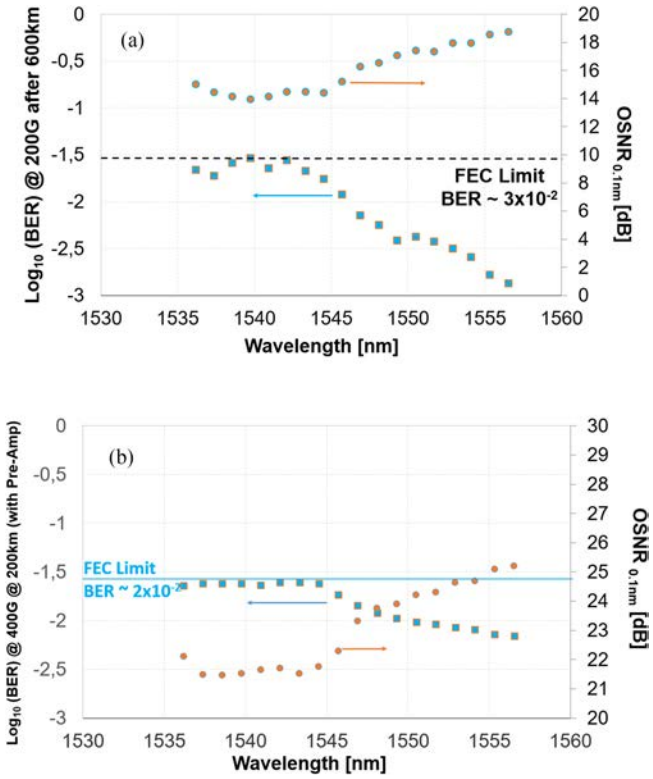

Fig. 15. BER and OSNR (in 0.1 nm) vs. wavelength (by step of 150 GHz) for (a) the 200G channel after 600 km and for (b) the 400G channel after 200 km (right) with the proprietary transponder in the serial configuration.

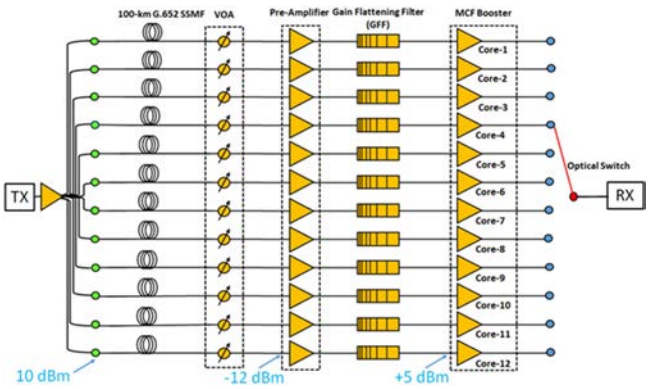

Fig. 16. Experimental set-up for the data center interconnect scenario at 400 G with twelve 100 km fiber spans in parallel. For measurement, an optical switch alternatively connects the receiver to the fiber links.

coupler stages (i.e., a first stage with 1:2 coupler and a second stage with two 1:8 couplers) split the signal in sixteen data flows, whose only twelve are used to feed the experiment. 10 dBm input power are sent in each of the twelve 100 km G.652 compliant fiber links. After crossing a VOA (allowing us to control the gain flatness of the MC-EYDFA) the data flow is amplified into one specific core of the MC-EYDFA. An optical switch connects the receiver previously presented to one of the twelve DCI fiber links.

Fig 17 presents the performance (i.e., BER and OSNR) of both 400G channels injected in the twelve transmission links

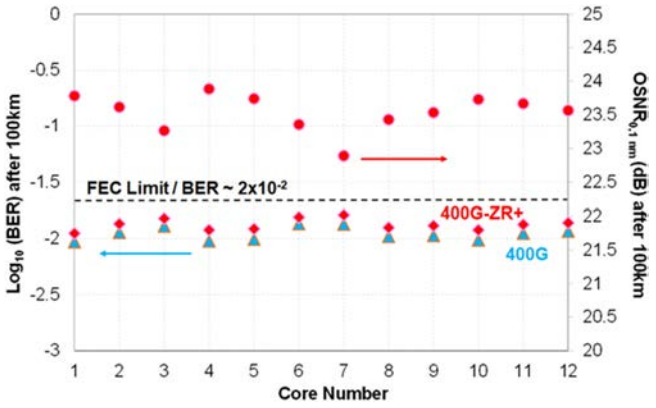

Fig. 17. BER and OSNR (in 0.1 nm) of the 400G signals (both 400G-ZR+ and 400G proprietary) versus the core number after 100 km DCI fiber links.

as a function of the core chosen inside the MC-EYDFA. The BER and OSNR (in 0.1 nm) of both 400G signals are nearly identical whatever the core considered inside the MC-EYDFA. The BER of 400G signals is, for each core, better than the FEC threshold (BER $\sim 2.10^{-2}$) ensuring the good working of the twelve DCI links considered here. From its side, OSNR in 0.1 nm is measured in the [23–24] dB range for the various links. This experiment clearly shows the potential of using MC-EYDFA in a DCI scenario where lot of capacity must be carried.

B. Use Cases for Multi-Core Optical Amplifier

This section lists the main use cases of MCF amplifiers in the context of long haul point to point optical WDM transmission [40] using single fiber bundles for reducing system power and complexity or the weakly coupled multi-core fiber (WC-MCF) systems. MC-EYDFA could be shared by WDM systems deployed fully or partially on the same site and cable infrastructures. In practical terms, Multi-Core Fiber (MCF) amplifiers packaged in equipment cards would be used in sites to amplify different optical multiplexed signals originated from different terminal equipment and propagating in different line fibers and possibly different cables. The mutualization of the amplification function can be envisaged if the different systems have compatible link engineering. From a link point of view, MCF amplifier sharing allows WDM system bundling. Although, in-line Reconfigurable Optical Add Drop Multiplexers (ROADM) can also be considered, point-to-point full WDM bundling, i.e. sharing MCF amplifiers among WDM systems on the same site infrastructure from site A to site B is an interesting use case.

1) Point to Point Full WDM Bundling: This case is a point to point full WDM bundling, i.e. sharing MCF amplifiers among WDM systems on the same site infrastructure from site A to site B. This case deals indeed with parallel WDM systems sharing their amplifiers. These parallel links are usually engineered the same way. This case is called point to point and can be divided into two subcases: The unidirectional case where MCF amplifiers are used to amplify optical multiplexed signals propagating in the same link direction. The bidirectional case where MCF

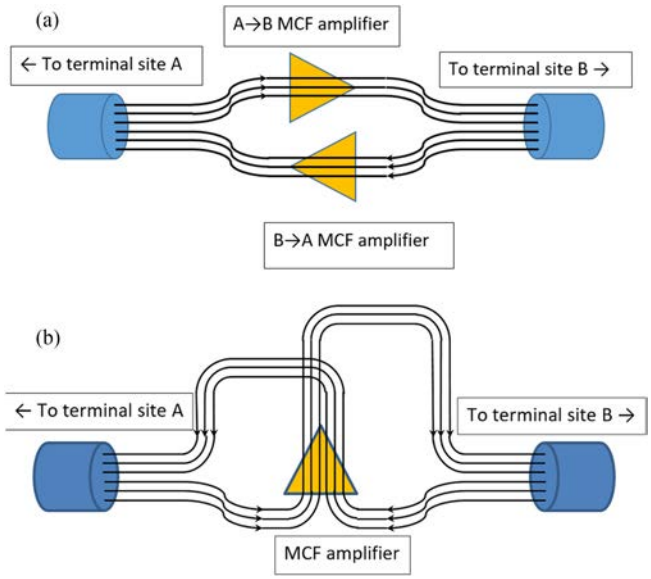

Fig. 18. (a) Unidirectional and (b) Bidirectectional use of MCF amplifiers.

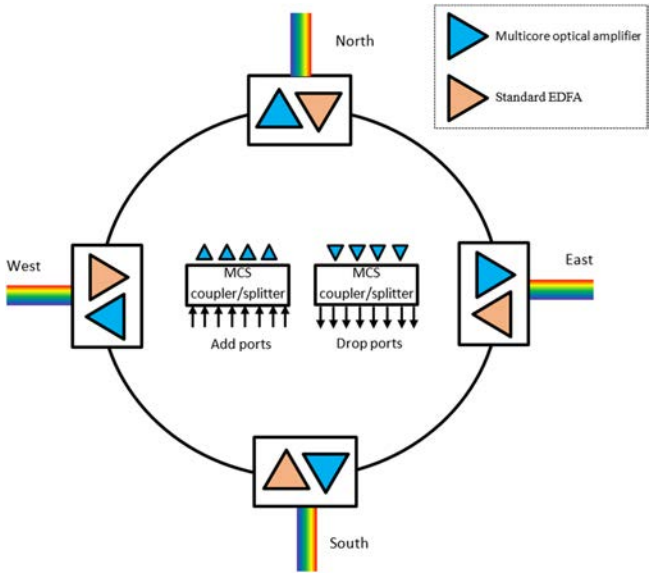

Fig. 19. Use of MCA in ROADM architecture.

amplifiers are used to amplify optical multiplexed signals propagating either in the same or in the opposite link direction. As reported in [41]–[42] the interleaving of propagation-directions in the MCF leads to a core to core crosstalk power below the ASE floor while keeping noise and gain characteristics unchanged. Thus, at least 3 dB reduction of total crosstalk power in the bidirectional case is expected, allowing an extended transmission distance with respect to the unidirectional case. Fig. 18 presents the two considered scenarios.

2) ROADM Amplification: In this section, we describe a typical use case of MCF amplifier in a ROADM architecture. The role of a WDM transport network is to carry optical channels corresponding to a specified traffic matrix. The network consists in nodes (also called sites) connected to each other through sections of optical fiber. Several types of nodes can be distinguished like terminal site, ROADM site and amplifier sites. The main attributes of a ROADM node are the Number of degrees, the Number of add/drop ports and its configuration (colored/colorless, Directed/Directionless and Contentioned/Contentionless. We consider the architecture prompted by the "open ROADM Multi-Source Agreement (MSA)" [43]. We take the example based on multicast switch architecture, a use case for 12-core EYDFA within a 4-degree ROADM having 64 add/drop ports is as follows:

- 4 cores as Boosters with 14 dB gain.
- 4 cores to compensate for the add Multi-Cast Switch (MSC) with 14 dB gain.
- 4 cores to compensate for the drop MCS with 14 dB gain.

The 14 dB gain is justified by the 14 dB insertion loss for the pass-through channels (compensated by a single stage amplification) and the 28 dB insertion loss for the add channels (compensated by two stage amplification). Replacing the A/D structure of open ROADM case by a multicast switch, the architecture becomes contentionless in a functional and components point of view. However, this infrastructure is more expensive.

Fig. 19 illustrates the location of EDFA amplifiers within a 4-degree C/D/C ROADM. The 4 amplifiers colored in red are pre-amplifiers and follow the specification for in-line amplifiers. The 12 amplifiers colored in blue are dedicated to compensate for the internal losses within the ROADM node. If the gain required to compensate for the IL of pass-through channels is close to the gain required to compensate for the IL of the add/drop structure, the gain requirement for all the blue amplifiers is the same. The amplification could be therefore advantageously mutualized with a multi-core amplifier to reduce the equipment cost, space and energy consumption. Indeed, the multiple boards of independent single-core EDFA would be replaced by a single board multi-core EYDFA equipped with a single pump laser. However, fine dynamic gain equalization still remains to be handled on a per fiber basis using WSS or DGE devices, depending on the ROADM's internal architecture.

C. Use of Multi-Core Amplifier for Cost and Energy Saving

In this section we report the techno-economic impact of 12-core Erbium-Ytterbium doped fiber amplifiers used in optical transport networks in terms of optical amplification equipment cost (CAPEX) and power consumption (OPEX) [44]. For the transmission analysis, we selected a loop of ∼2230 km in the French domestic core transport network (between Paris and Marseille) composed of 7 links with 29 EDFAs and 8 ROADMs having from 2 to 5 degrees.

Table IV gives for each of the 7 links that connect two successive ROADMs, the link length, the fiber filling ratio @ T0 (considering WDM systems with 80 channels at 100G in the C-band and a fixed optical channel grid of 50 GHz) and the number of amplification sites. We considered at T0 (2018) only one operated pair of fibers (one for each of the two directions). By multiplying the filling ratio of each link with the total capacity of the WDM system, the link throughput can be inferred. Then we extrapolate the capacity needed for the

TABLE IV
NETWORK TOPOLOGY WITH THE FIBER FILLING RATIO

Network Link	Length (km)	Fiber Filling Ratio (%)	Ampl. Site
A	570	60	8
B	409	90	4
C	127	80	2
D	242	50	3
E	253	90	4
F	248	100	3
G	352	80	5

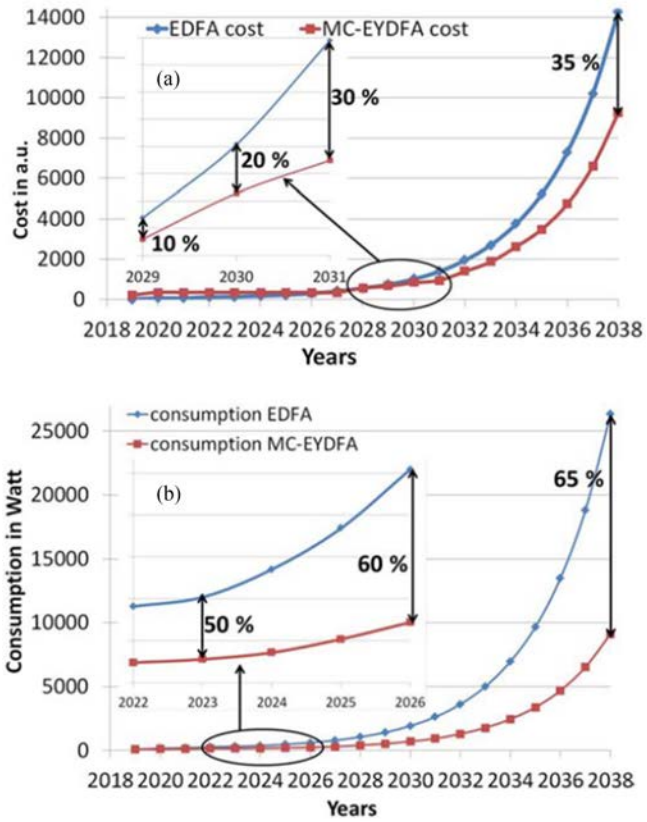

Fig. 20. Cumulated costs for in line EDFAs/MC-EYDFAs.

up-coming period (i.e. from T0 up to 2038) considering a 40% yearly traffic growth. Knowing the capacity for each new year, we calculate the number of WDM channels to be switched on and the corresponding number of fibers to light up, depending on the bandwidth requirements of EDFA or MC-EYDFA and the assumed transmission technique.

For cost comparison, we consider a reference cost of 1 arbitrary unit (a.u) for the standard EDFA. The MC-EYDFA cost is conservatively fixed at 6 a.u as we should expect at least a 50% cost reduction from pump sharing. Under these cost and traffic growth assumptions, Fig. 20 shows the evolution of the cumulated costs and energy consumption for line EDFAs / MC-EYDFAs [45]. From this study, we can see that that 35% and 33% cost savings can be achieved by year 2038 if we decide to use MC-EYDFAs in our transport network. In terms of energy consumption, the reduction can reach 60% as early as 2026. Even if the amplifiers cost is often masked by the cost of WDM transceivers, this study shows that several tens of millions of Euros can be saved by the replacement of EDFAs.

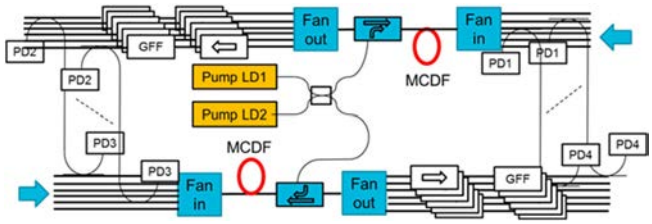

Fig. 21. Architecture of a submarine repeater using multi-core amplifiers (6 fiber pairs) (PD: Photodiode - MCDF: Multi-Core Doped Fiber).

D. Perspective of Multi-Core Amplifier for Submarine Systems

The capacity of long submarine links is limited by the electrical power that can be transferred to repeaters from the onshore Power Feeding Equipment (PFE) [46]. Hence, multi-core amplifiers with shared pumping are of first interest in the context of submarine links as they exhibit very good power efficiency. The first driver for applying multi-core amplifiers to long haul submarine links is the strong electrical power constraint, both in terms of current and voltage [47]. Such technology is about to improve the efficiency of optical amplifiers in terms of electrical to optical power conversion ratio, thus paving the road to energy savings or more capacity for the same amount of power. The repeater architecture is as shown in Fig. 21. Due to the low gain operation, no hybrid structure based on a combination of single core EDFA and multi-core amplifier stage is necessary. The multi-core doped fiber is now shared among several fibers with optical FIFO couplers. As for single core designs, forward and backward-propagating pumping schemes are possible. The gain flattening filters as well as optical isolators are not shared. So are monitoring devices that have to be implemented for every fiber.

In [48] we have studied the feasibility of using MC-EYDFA for such submarine application. As subsea typical span length is ∼50–70 km [47], with a fiber attenuation of 0.16 dB/km, the amplifier have to compensate a typical span loss in 10 and 15 dB range. To design this amplifier, we used the same algorithm and simulation tool presented in Section III. Results show that amplifier need to be designed with a different active fiber length and ions concentration ratio as 6 m and 30 respectively, compared to 5.5 and 20 for the architecture describe in Section V-A.

Fig. 22 gives simulation results in terms of gain and NF considering different forward pump power for a given backward value. In term of NF, a 6.9 dB @1550 is achievable considering an extended bandwidth from 1538 to 1570 nm. We can see that, for submarine application, such amplifier can be similarly designed and give good results even if we observe NF degradation.

We then propose to compare the performance of the optimized MC-EYDFA and of a standard EDFA in similar conditions of operation and optimization: +5 dBm core total input power and identical total gain after equalization, 8.8 dB including Fan-In

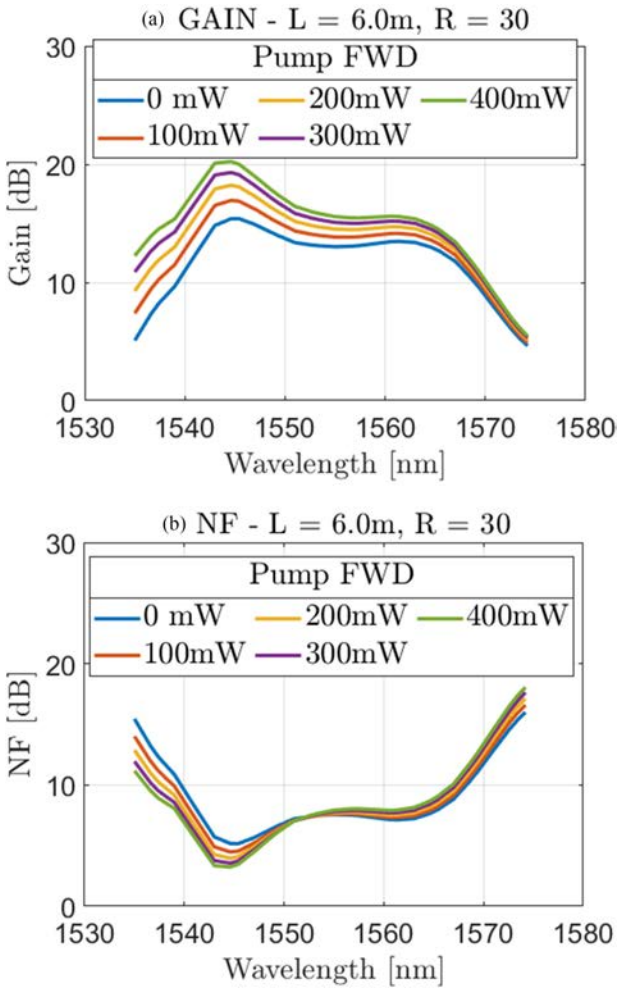

Fig. 22. (a) Gain and (b) NF versus wavelength for the considered extended C-band - Active fiber length: 6 m, Concentration ratio: 30.

Fan-Out, splice Losses, pump combiner losses and a perfect Gain Flattening Filter.

Table V summarizes the assumed parameters as well as the resulting optical amplifier features in terms of bandwidth, doped fiber gain (mean, and minimum, the latter corresponding to gain after equalization), average doped fiber noise figure, equivalent noise figure, total output power, and required total optical/electrical pump powers, assuming an electro-optic efficiency of 25% for core-pump EDFA laser diode and 50% for cladding-pump EYDFA broad area laser diode. This allows to compare the raw amplifier power efficiency ρ_{EO}, defined as the ratio of total output optical power over total electrical pump power. The EYDFA is 2.9x more power-efficient than the EDFA. However, since quality of transmission indeed depends on signal to noise ratio [47], it is fair to correct raw power efficiency by the average noise figure degradation with respect to a typical EDFA (∼4.5 dB). We define this parameter as $\rho_{EO,corr} = \rho_{EO,eq} \times NF_{EDFA,ref}/NF$. Beyond intuition, the achievable information rate per Watt of a multi-fiber/core transmission link can be shown proportional to this $\rho_{EO,corr}$ parameter and a factor depending on the degree of parallelism of the link [49]. Then, the corrected power efficiency of the EYDFA is

TABLE V
SIMULATION RESULTS FOR SUBMARINE APPLICATION

Parameters	MC-EYDFA	EDFA	Unit
N_{core}	12	1	
Signal Input Power	+5	+5	dBm
WDM Channels	48	48	
Pump Combiner Loss	0.1	0.5	dB
Signal Loss (In / Out)	0.5 / 0 .5	0.2 / 0.1	dB
Gain (Min / Mean)	9.8 / 12.3	9.1 / 11	dB
Module Gain	8.8	8.8	dB
NF Doped Fiber	7.9	4.3	dB
NF_{eq}	8.4	4.5 (NF_{ref})	dB
Per core Out. Pow.	13.8	13.8	dBm
Pump Power (Opt / Elec)	7.2 / 14.4	0.8 / 3.8	W
ρ_{EO}	0.5	0.25	%
$\rho_{EO,eq}$ $\left(\frac{P_{out,core} \times \rho_{EO}}{P_{pump,opt}/N_{core}}\right)$	2	0.8	%
$\rho_{EO,corr}$ $\left(\rho_{EO,eq} \times \frac{NF_{ref}}{NF_{eq}}\right)$	0.8	0.8	%

comparable to that of an EDFA, 0.8%, pending consolidated assumptions.

Such preliminary results are promising. The potential of such amplifier in term of cost, energy and space saving is very interesting but involves penalty on system performances due to degraded NF. It could probably represent an interesting alternative for medium-reach submarine cables.

VI. CONCLUSION

This paper has presented the implementation of an all-fiberized 12c-EYDFA prototype.

In the first part we have developed the considered multi-core optical amplifier technology in term of architecture assembly. The prototype is based on 12 single mode core with circular arrangement.

In order to determine the optimal fiber parameters and to predicted the performance and behavior of a multi-core Er^{3+}/Yb^{3+} amplifier, a simulation tool has been used. The model is based on classical two levels Er/Yb transfer energy system. Er/Yb doped fiber length, ratio of concentration and optimum pump powers have been studied. Results in term of gain, noise figure and gain variation have been obtained. As minimizing the amplifier noise figure imply decreasing the average gain and increasing the gain variation, a pseudo swarm optimization algorithm has been proposed to find a trade-off. The best compromise point that maximize the gain, minimize the noise figure and gain variation has been found.

Based on these recommendations, the active Er/Yb doped fiber has been realized and implemented on the MC-EYDFA prototype. First characterizations as gain, noise figure and per

core output power have been measured and compared with simulations showing a good agreement. Thanks to the optimized design and manufacturing processes, core-to-core spacing of the active fiber and 12+1 combiners matches very accurately. Splicing procedure enables an average splice loss of ∼0.5 dB. An average gain of 20 dB in the C-band for an input power per core of 1mW is achieved with 5.3W of pump power at 940 nm with an optical power conversion of 23%.

We then used the designed amplifier in WDM transmission system. We showed the large application range of a 21-dBm/core for 200G/400G LH, metro/regional and DCI transport networks with ROADM. Even if its bandwidth is reduced compared to a standard EDFA, the 12c-EYDF amplifier presents a total power consumption of 11 Watts (i.e. 4-fold less than twelve standard EDFAs). After that, we have presented different application scenario including multi-core amplifier for point to point full WDM bundling or ROADM amplification. The techno-economic study has shown the advantage of such technology by reducing of 35% and 60% of the cost and energy consumption respectively.

Finally, we have proposed the use of multi-core amplifier for submarine applications. We have studied the extension of the considered optical bandwidth and have obtained a low degradation of the gain variation and NF, only 0.2 dB penalty @1550 nm considering 1538–1575 nm, compared to traditional 1535–1565 nm. Nevertheless, it add the possibility of using the same amplifier for red-shifted bandwidth (towards the L-band). Comparison between standard EDFA based on a new criteria has been proposed. It results that information rate per Watt for MC-EYDFA is proportional to the proposed corrected power efficiency and a factor depending on the degree of parallelism. Furthermore, corrected power efficiency of the MC-EYDFA is comparable to that of an EDFA.

There is still room for improvement of the amplifier performances by further optimizing cleaving/splicing procedures and combining co- and counter-directional pumping. Based on power consumption comparisons, this prototype demonstrates the benefit of pump mutualization though multi-core fiber technology. Estimated power reduction compared to 12 EDFAs reaches a fourfold factor, leading to potential breakthroughs in the domain of mutualized amplifiers for ROADM and SDM transmission applications. Further developments should allow having two amplification stages based on MCF and a GFF directly printed inside the MCF. In addition to potential cost energy and footprint savings, results are promising.

REFERENCES

[1] R.-J. Essiambre and R. W. Tkach, "Capacity trends and limits of optical communication networks," *Proc. IEEE*, vol. 100, no. 5, pp. 1035–1055, May 2012.

[2] P. J. Winzer and D. T. Neilson, "From scaling disparities to integrated parallelism: A decathlon for a decade," *J. Lightw. Technol.*, vol. 35, no. 5, pp. 1099–1115, Mar. 2017.

[3] B. J. Puttnam et al., "High capacity transmission systems using homogeneous multicore fibers," *J. Lightw. Technol.*, vol. 35, no. 6, pp. 1157–1167, 2017.

[4] K. Imamura, K. Mukasa, and T. Yagi, "Effective space division multiplexing by multicore fibers," in *Proc. 36th Eur. Conf. Exhibit. Opt. Commun.*, 2010, pp. 1–3.

[5] K. Igarashi, T. Tsuritani, I. Morita, and M. Suzuki, "Ultra long haul high capacity super Nyquist WDM transmission experiment using multicore fibers," *J. Lightw. Technol.*, vol. 33, no. 5, pp. 1027–1036, 2015.

[6] R. Ryf et al., "Mode-division multiplexing over 96 km of few-mode fiber using coherent 6× 6 mimo processing," *J. Lightw. Technol.*, vol. 30, no. 4, pp. 521–531, 2012.

[7] R. Ryf et al., "High-spectral-efficiency mode-multiplexed transmission over graded-index multimode fiber," in *Proc. Eur. Conf. Opt. Commun.*, 2018, pp. 1–3, doi: 10.1109/ECOC.2018.8535536.

[8] K. Shibahara et al., "Dense sdm (12-core x 3-mode) transmission over 527 km with 33.2-ns mode-dispersion employing low-complexity parallel MIMO frequency-domain equalization," *J. Lightw. Technol.*, vol. 34, no. 1, pp. 196–204, 2016.

[9] R. Ryf et al., "Coupled-core transmission over 7-core fiber," in *Proc. Opt. Fiber Commun. Conf.*, 2019, Paper Th4B–3.

[10] S. Jain et al., "32-core inline multicore fiber amplifier for dense space division multiplexed transmissionsystems," in *Proc. 42nd Eur. Conf. Opt. Commun.*, 2016, pp. 1–3.

[11] E. L. T. de Gabory, H. Takeshita, K. Matsumoto, and S. Yanagimachi, "Reduction in power consumption in multi-core amplifier," in *Proc. Opt. Fiber Commun. Conf.*, 2019, pp. 1–3.

[12] H. Ono et al., "12-core double-clad ER/YB-doped fiber amplifier employing free-space coupling pump/signal combiner module," in *Proc. 39th Eur. Conf. Exhib. Opt. Commun.*, 2013, pp. 1–3, doi: 10.1049/cp.2013.1469.

[13] K. Takeshima et al., "51.1-Tbit/s MCF transmission over 2,520 km using cladding pumped 7-core EDFAs," in *Proc. Opt. Fiber Commun. Conf.*, 2015, Paper W3G–1, doi: 10.1364/OFC.2015.W3G.1.

[14] G. Le Cocq et al., "Few mode ER3 -doped fiber with micro-structured core for spatial division multiplexing," in *Proc. Workshop Specialty Opt. Fibers Appl.*, 2013, Art. no. W3.1.

[15] K. S. Abedin et al., "Cladding-pumped erbium-doped multicore fiber amplifier," *Opt. Exp.*, vol. 20, no. 18, pp. 20191–20200, 2012.

[16] C. Matte-Breton, R.-J. Essiambre, C. Kelly, Y. Messaddeq, and S. LaRochelle, "Multicore cladding-pumped fiber amplifier with annular erbium doping for low gain compression," *J. Lightw. Technol.*, vol. 40, no. 6, pp. 1836–1846, 2022, doi: 10.1109/JLT.2022.3144940.

[17] J. E. Townsend, W. L. Barnes, and S. G. Crubb, "Yb3 sensitised Er3+ doped silica optical fibre with ultra high transfer efficiency and gain," *MRS Online Proc. Library*, vol. 244, pp. 143–147, 1991.

[18] C. Matte-Breton et al., "Modeling and characterization of cladding-pumped Erbium-Ytterbium co-doped fibers for amplification in communication systems," *J. Lightw. Technol.*, vol. 38, no. 7, pp. 1936–1944, Apr. 2020, doi: 10.1109/JLT.2019.2961061.

[19] E. Gueorguiev, "Conception et réalisation d'amplificateurs de forte puissance à base de fibre dopée erbium et erbium-ytterbium double gaine fonctionnant en régimes continu et impulsionnel," Ph.D. dissertation, Paris, France, Eccole Nationale Supérieure des Telecommunication, 2009.

[20] K. S. Abedin et al., "Amplification and noise properties of an Erbium-doped multicore fiber amplifier," *Opt. Exp.*, vol. 19, no. 17, pp. 16715–16721, 2011.

[21] N. K. Fontaine et al., "Coupled-core optical amplifier," in *Proc. Opt. Fiber Commun. Conf.*, 2017, pp. 1–3.

[22] M.-J. Li, B. Hoover, V. N. Nazarov, and D. L. Butler, "Multicore fiber for optical interconnect applications," in *Proc. 17th Opto- Electron. Commun. Conf.*, 2012, pp. 564–565.

[23] B. Zhu et al., "Seven-core multicore fiber transmissions for passive optical network," *Opt. Exp.*, vol. 18, no. 11, pp. 11117–11122, 2010.

[24] P. Glas, M. Naumann, A. Schirrmacher, and T. Pertsch, "The multicore fiber–a novel design for a diode pumped fiber laser," *Opt. Commun.*, vol. 151, no. 1–3, pp. 187–195, 1998.

[25] M. Yamada, H. Ono, N. Sakai, K. Takenaga, and S. Matsuo, "Theoretical study of crosstalk characteristics for multi-core optical fiber amplifiers," in *Proc. Opt. Fiber Commun. Conf.*, 2013, pp. 1–3.

[26] G. Mélin et al., "Power efficient all-fiberized 12-core erbium/ytterbium doped optical amplifier," in *Proc. Opt. Fiber Commun. Conf.*, 2020, pp. 1–3.

[27] C. Jin, B. Ung, Y. Messaddeq, and S. LaRochelle, "Annular-cladding Erbium doped multicore fiber for SDM amplification," *Opt. Exp.*, vol. 23, no. 23, pp. 29647–29659, 2015.

[28] E. Desurvire and M. N. Zervas, "Erbium-doped fiber amplifiers: Principles and applications," *Phys. Today*, vol. 48, no. 2, 1995, Art. no. 56.

[29] Y. Jaouën, S. Bordais, E. Olmedo, G. Kulcsar, and J.-Y. Allain, "High power cladding-pumped er3/yb3 fiber amplifiers: Technologies, performances and impact of nonlinear effects," *Annales des Télécommunications*, vol. 58, no. 11, pp. 1640–1666, 2003.

[30] P. F. Wysocki, J. L. Wagener, M. J. Digonnet, and H. J. Shaw, "Evidence and modeling of paired ions and other loss mechanisms in erbium-doped silica fibers," in *Proc. SPIE*, vol. 1789, pp. 66–79, 1993.
[31] L. DASHENG, "Multi objective particle swarm optimization: Algorithms and applications," 2009. [Online]. Available: https://scholarbank.nus.edu.sg/handle/10635/16724
[32] F. Marini and B. Walczak, "Particle swarm optimization (PSO). a tutorial," *Chemometrics Intell. Lab. Syst.*, vol. 149, pp. 153–165, 2015.
[33] A. Lebreton et al., "Design optimization of 12 core er3 /yb3 co-doped amplifier and its experimental validation," in *Proc. Optoelectron. Commun. Conf.*, 2021, Paper T3C–4.
[34] J. Nilsson et al., "High-power wavelength-tunable cladding-pumped rare-earth-doped silica fiber lasers," *Opt. Fiber Technol.*, vol. 10, no. 1, pp. 5–30, 2004.
[35] Lumentum, "Pump lasers." Lumentum, 2022. [Online]. Available: https://www.lumentum.com/en/opticalcommunications/products/pump-lasers/14-pin-9xx-pump-lasers
[36] ITU, "ITU-T G.709.OTU4LR recommandation." [Online]. Available: http:/www.itu.int/itu-t/recommendations/rec.aspx?rec=13522&lang=en
[37] "OpenROADM_MSA3.01 W-Port Digital Specification.docx," 2019. [Online]. Available: http://www.OpenROADM.org
[38] "Openzr msa technical specifications." 2022. [Online]. Available: www.openzrplus.org/documents
[39] E. Pincemin et al., "12-core erbium/ytterbium-doped fiber amplifier for 200 g/400 g long-haul, metro-regional, DCI transmission applications with roadm," in *Proc. Eur. Conf. Opt. Commun.*, 2021, pp. 1–4, doi: 10.1109/ECOC52684.2021.9606073.
[40] D. Amar, P. Gravey, M. Morvan, M.-L. Moulinard, J. Thouras, and E. Pincemin, "Link engineering strategies for SDM amplification in conventional optical transport networks," in *Proc. Photon. Switching Comput.*, 2018, pp. 1–3.
[41] K. Maeda, S. Takasaka, K. Kawasaki, K. Yoshioka, R. Sugizaki, and M. Tsukamoto, "Propagation direction interleaved cladding pumped 19-core edfa," in *Proc. 24th OptoElectron. Commun. Conf. Int. Conf. Photon. Switching Comput.*, 2019, pp. 1–3.
[42] K. Maeda, S. Takasaka, K. Yoshioka, R. Sugizaki, M. Tsukamoto, and Y. Arashitani, "Propagation direction interleaved cladding pumped 19-core EDFA in L-band," in *Proc. Opto- Electron. Commun. Conf.*, 2020, pp. 1–3.
[43] "Openroadm msa," 2016. [Online]. Available: http://www.openroadm.org
[44] J. Thouras, E. Pincemin, D. Amar, P. Gravey, M. Morvan, and M.-L. Moulinard, "Introduction of 12 cores optical amplifiers in optical transport network: Performance study and economic impact," in *Proc. 20th Int. Conf. Transparent Opt. Netw.*, 2018, pp. 1–4.
[45] J. Thouras, E. Pincemin, D. Amar, P. Gravey, M. Morvan, and M.-L. Moulinard, "Economic impact of multicore Erbium Ytterbium doped fiber amplifier in long haul optical transport networks," in *Proc. Photon. Switching Comput.*, 2018, pp. 1–3.
[46] J. D. Downie, X. Liang, and S. Makovejs, "Examining the case for multicore fibers in submarine cable systems based on fiber count limits," *IEEE J. Sel. Topics Quantum Electron.*, vol. 26, no. 4, pp. 1–9, Jul./Aug. 2020.
[47] R. Dar et al., "Cost-optimized submarine cables using massive spatial parallelism," *J. Lightw. Technol.*, vol. 36, no. 18, pp. 3855–3865, Sep. 2018.
[48] A. Lebreton, Y. Jaouën, J.-C. Antona, and L. Chao, "Multi-core Erbium/Ytterbium doped fiber amplifier with extended bandwidth for submarine applications," in *Proc. Optoelectron. Commun. Conf.*, 2022, pp. 1–3.
[49] A. Bononi, J.-C. Antona, P. Serena, A. Carbo-Meseguer, and C. Lasagni, "The generalized droop model for submarine fiber-optic systems," *J. Lightw. Technol.*, vol. 39, no. 16, pp. 5248–5257, Aug. 2021.